

Two Allotropic Forms for the Poly(ethylene oxide)-Resorcinol Molecular Complex

E. Delaite, J.-J. Point, P. Damman, and M. Dosière*

Université de Mons-Hainaut, Département des Matériaux et Procédés, Place du Parc, 20, B-7000 Mons, Belgium

Received January 14, 1992; Revised Manuscript Received April 20, 1992

ABSTRACT: Differential scanning calorimetry indicates that the poly(ethylene oxide)-resorcinol molecular complex crystallizes into two allotropic forms, denoted here as α and β forms, respectively. The phase diagram of the PEO-resorcinol system, involving only the already known allotropic α form of the molecular complex, is obtained by differential scanning calorimetry. The α form of the molecular complex crystallizes as unbanded spherulites. The reflections of the wide-angle X-ray patterns from stretched film and spherulites of the α form are indexed on the basis of an orthorhombic unit cell ($a = 1.050$ nm, $b = 1.013$ nm, $c = 0.9776$ nm), with the $Pna2_1$ space group. This unit cell differs widely from the monoclinic unit cell previously reported by Myasnikova et al. As shown from polarized FTIR spectroscopy, the 2-5 axis of the resorcinol molecule is parallel to the a^* reciprocal parameter of the unit cell of the molecular complex. The benzene ring of the resorcinol molecule is nearly perpendicular to the c crystallographic parameter. The new allotropic form of the poly(ethylene oxide)-resorcinol molecular complex (β form) crystallizes as banded spherulites. This β form of the molecular complex is also studied by differential scanning calorimetry, optical microscopy, and Fourier transform infrared spectroscopy. The determination of the unit cell for the β form of the PEO-resorcinol molecular complex is still in progress.

Introduction

Poly(ethylene oxide) (PEO) forms various crystalline molecular complexes with organic^{1,2} and inorganic³⁻⁷ molecules such as urea, thiourea, mercuric chloride, and sodium iodide. Crystalline complexes with PEO as host and *p*-dihalogenobenzene compounds as guest molecules have been recently discovered and investigated in our laboratory.⁸⁻¹² The heat of formation of the *p*-dichlorobenzene-PEO complex was found to be very low (4000 J/mol of *p*-dichlorobenzene), and the association between PEO and *p*-C₆H₄Cl₂ molecules is physical. The present study deals with other molecular complexes of PEO and dihydroxybenzene molecules, in which the interactions between the host and guest components are greater. The occurrence of a PEO-resorcinol molecular complex has been already reported by Myasnikova et al.¹³ and Cheng et al.¹⁴ The phase diagram shows that a bell-shaped region, centered around a 2:1 stoichiometry (i.e. two PEO monomer units for one resorcinol molecule), which separates two eutectic points.¹³ From an X-ray investigation, Myasnikova et al. proposed a monoclinic unit cell: $a = 1.605$ nm, $b = 1.425$ nm, $c = 0.984$ nm, $\beta = 112^\circ$ and space group, $P2_1/a$. This unit cell contains two chains, eight PEO monomer units and four resorcinol molecules.¹³

In this paper, we report that differential scanning calorimetry indicates this crystalline complex has two allotropic modifications: the reported form (hereafter " α form") and a new allotropic form (hereafter " β form"). Both these allotropic forms of the PEO-resorcinol molecular complex are investigated by differential scanning calorimetry, optical microscopy, X-ray diffraction, and Fourier transform infrared spectroscopy. The wide-angle X-ray pattern of the metastable β form is presently not available taking into account a lifetime at room temperature shorter than 0.5 h. A study of the transformation kinetics from the metastable β form to the stable α form is still in active progress.

Experimental Section

Poly(ethylene oxide) (PEO) of low molar mass ($M_w = 6000$) was obtained from Hoechst. Low molar mass deuterated PEO

($M_w = 2000$) was purchased from MSD Isotopes (Montreal). High molar mass samples ($M_w = 5 \times 10^6$) and resorcinol were purchased from Aldrich and Merck, respectively.

Spherulitic samples of the α and β forms of the PEO-resorcinol molecular complex used for polarized optical microscopy were crystallized in the form of films, 20 μ m thick, previously quenched from the melt in liquid nitrogen. Spherulitic films of the α form of the PEO-resorcinol molecular complex, used in X-ray diffraction, were supported between sheets of polypropylene inserted between two glass slides. The molar mass M_w of the PEO sample used for these purposes was 6000. Oriented films of the α form were prepared by stretching at room temperature, a quenched film of the PEO-resorcinol molecular complex of high molar mass PEO ($M_w = 5 \times 10^6$).

A Perkin-Elmer differential scanning calorimeter (DSC4 Model), fitted with a TADS computing station and a low-temperature cooling accessory, was used for measurement of the phase transitions. Sealed aluminum caps for volatile samples containing approximately 5 mg of sample were used. The scanning rate was 5 K/min. Indium was used for calibration of temperature and power scales. Optical observations were made on an Ortholux microscope (Leitz), fitted with a Mettler FP52 hot stage. The wide-angle X-ray pattern of the α spherulitic form of the molecular complex was taken at the peripheral part of a large spherulite. Infrared spectra were recorded with a Bruker IFS 113V Fourier transform infrared spectrometer, 32 coadded interferograms were scanned with a resolution of 2 cm⁻¹.

Results and Discussion

Two Allotropic Forms for the PEO-Resorcinol Molecular Complex. Figure 1 shows different melting curves obtained for the PEO-resorcinol molecular complex, having the same stoichiometry (CH₂CH₂O)_{2x}(C₆H₄(OH)₂)_x. The first DSC curve shows two endotherms due to the melting of the two allotropic forms of the molecular complex noted as β and α , respectively (Figure 1a). Parts b and c of Figures 1 show the melting curves of both pure allotropic forms, i.e., the β and α phases, respectively. The melting temperatures of the β and α phases of the molecular complex are 71 and 93 °C, respectively. The heat of fusion of the molecular complex (α form) is 155 J/g. The fact that two different allotropic forms are actually involved is documented later in this paper.

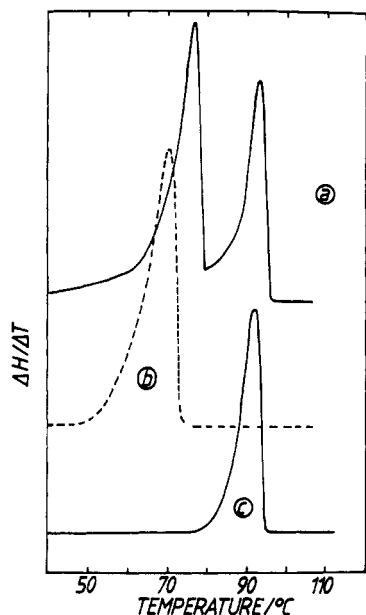


Figure 1. DSC curves of PEO-resorcinol complexes having the stoichiometric composition $(\text{CH}_2\text{CH}_2\text{O})_{2x}(\text{C}_6\text{H}_4(\text{OH})_2)_x$ showing the melting of a mixture of β and α phases (a), the β phase (b), and the α phase (c).

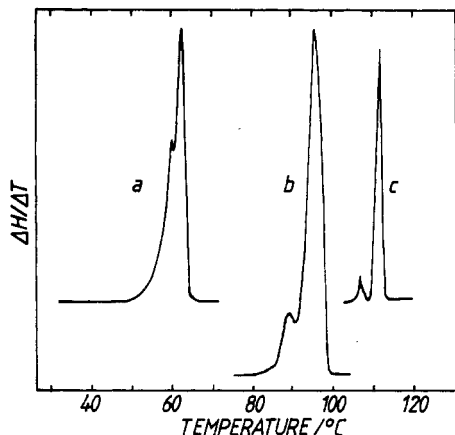


Figure 2. Melting curves of PEO (a), molecular complex (b), and resorcinol (c).

Stable Form of the PEO-Resorcinol Molecular Complex (α Form). Phase Diagram of the PEO-Resorcinol 2:1 Molecular Complex. The melting curves of pure PEO ($M_w = 6000$), resorcinol, and the α form of the molecular complex are given in Figure 2. The melting curve of pure PEO given in Figure 2a shows two endotherms: the main peak at 61.5 °C due to the melting of extended chain PEO crystals and the shoulder at 59 °C due to the melting of once folded crystals are in good agreement with previously reported data equal respectively to 63.3 and 60.7 °C.¹⁵ The melting curve of pure resorcinol shows two endotherms, one at 106.7 and the other at 111.8 °C, which are respectively due to the two allotropic forms of resorcinol.¹⁶ Resorcinol when cocrystallized with the molecular complex phase appears to be in the high melting form. The two endotherms observed in the melting curve of the α form of the PEO-resorcinol molecular complex, may result from the melting of PEO complex crystals with extended chains and once folded chains, respectively.

The phase diagram is shown in Figure 3. The molar fraction of resorcinol and the melting temperature are 0.10 and 43 °C, respectively, for the first eutectic and 0.49 and 86 °C for the second eutectic point.

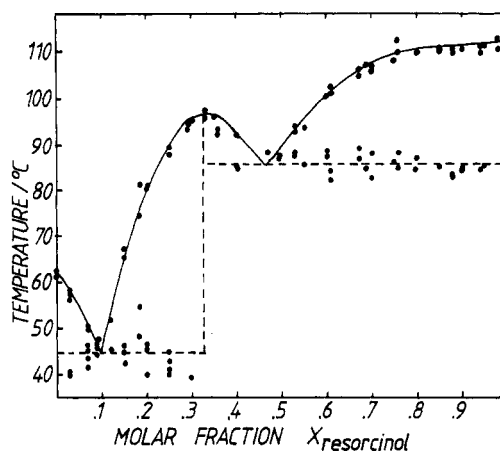


Figure 3. Phase diagram of the PEO-resorcinol system (α form).

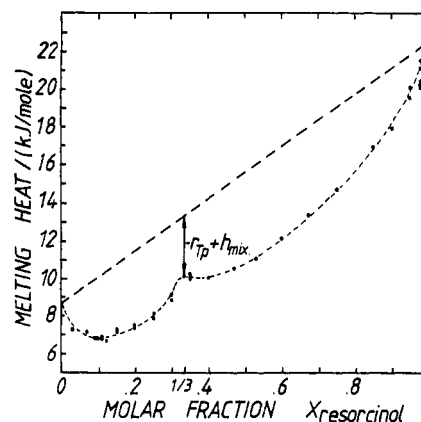


Figure 4. Heat of melting for various mixtures of PEO and complex or of a mixture of resorcinol and complex versus the molar fraction of resorcinol.

Heat of Mixing and Heat of Reaction for the Complexation Reaction. Figure 4 shows the total heat of fusion for mixtures of PEO-resorcinol previously comelted, homogenized, and recrystallized versus the molar fraction of resorcinol. The experimental data are distributed on two branches, giving a cusp point at their intercept for a resorcinol molar fraction of resorcinol of 0.33, i.e. the stoichiometric ratio of the molecular complex. Such behavior is expected if the heat of formation (noted r_{Tp}) of the solid complex from solid components and the heat of mixing of liquid components Δh_{mix} are both different from zero. The complexation from the solid components is exothermic because the cusp point is upward.

Successive melting traces of a stoichiometric physical mixture of resorcinol and PEO are shown in Figure 5. In the first DSC trace (Figure 5a), the first endotherm (59 °C) is due to the fusion of PEO. At higher temperatures, we observe successively a partial complexation of the resorcinol, the melting of unreacted resorcinol, and lastly the melting of the molecular complex. The heats of fusion in the successive scans are given in Table I. The probable nonhomogenization of the liquid phase after the first melting may explain why the absorbed heat increases progressively. The difference between the heat of fusion of the complex (containing 2 mol of PEO monomer and 1 mol of resorcinol) (30.70 kJ) and the experimental value for the heat of cofusion of a physical mixture containing 1 mol of resorcinol and 2 mol of PEO monomers (20.54 kJ) is the heat of formation r_{Tp} of the molecular complex which is equal to 10.16 kJ/mol of complex. The difference between the sum of the molar heat of fusion of resorcinol (22.46 kJ/mol) and the heat of fusion of a two monomeric mole unit of PEO (17.29 kJ/mol), and the heat of cofusion

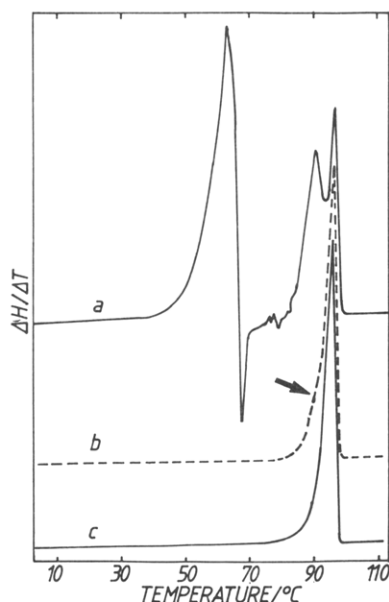


Figure 5. Successive DSC traces for a sample of PEO and resorcinol in stoichiometric proportion. The heating rate was 5 °C/min. The preparation was cooled to 0 °C after each run. In the first run, the sample is a mixture of resorcinol crystals and PEO. In the second run (b), the melting peak of the molecular complex presents a slight shoulder, shown by the arrow, indicating that the sample did not contain only the molecular complex (α form) even after a first melting in the calorimeter.

Table I
Heat of Fusion of PEO-Resorcinol in Stoichiometric Proportion^a

| experiment | first run | second run | third run | last run |
|------------|-----------|------------|-----------|-----------|
| 1 | 7449 | 9635 | 9919 | 10367 (7) |
| 2 | 6847 | 9521 | 9723 | |
| 3 | 7119 | 9027 | 9443 | 9556 (4) |
| 4 | 6931 | 9515 | 9511 | |

^a Melting heats are given in Joules per mole of molecular complex ($1/3$ mol of resorcinol, $2/3$ mol of monomer unit of PEO). The first run corresponds to the melting of a physical mixture. The subsequent runs correspond approximately to the melting of the complex (see text).

of the same system (20.54 kJ) gives an estimation of the heat of mixing for the liquid components $\Delta h_{\text{mix}} = -19.20$ kJ (per mole of complex or for 3 mol of the mixture). Both these values for the heat of reaction and the heat of mixing are most likely underestimated, because in the reported experiment, the melt obtained after the first melting of the physical mixture of the two components was probably not a homogeneous solution.

Optical Microscopy. Figure 6 is an optical micrograph, showing several unbanded spherulites of the PEO-resorcinol molecular complex (α form). Between crossed polaroids, these spherulites reveal a dark Maltese cross pattern along the vibration directions of the polarizer and analyzer.¹⁷ The spherulites are negatively birefringent. The melting temperature of unbanded spherulites, determined from optical microscopy, ranges from 93 to 95 °C in close agreement with data obtained from DSC measurements (Figure 1c).

X-ray Diffraction. X-ray diffraction patterns exhibiting fiber type orientations have been obtained from two types of samples of the PEO-resorcinol molecular complex (α form): stretched films and unbanded spherulites. The orientation characteristics of the patterns are discussed below.

Stretched Films. The wide-angle X-ray pattern of a stretched sample of the PEO-resorcinol molecular complex

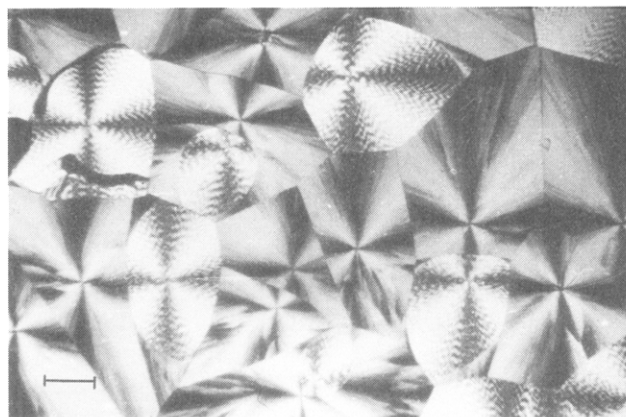


Figure 6. Optical micrograph (crossed polaroids) showing mainly unbanded spherulites of a PEO-resorcinol complex obtained from crystallization from the melt between two glass covers. The scale bar is 200 μm . The PEO molecular weight is 6000.

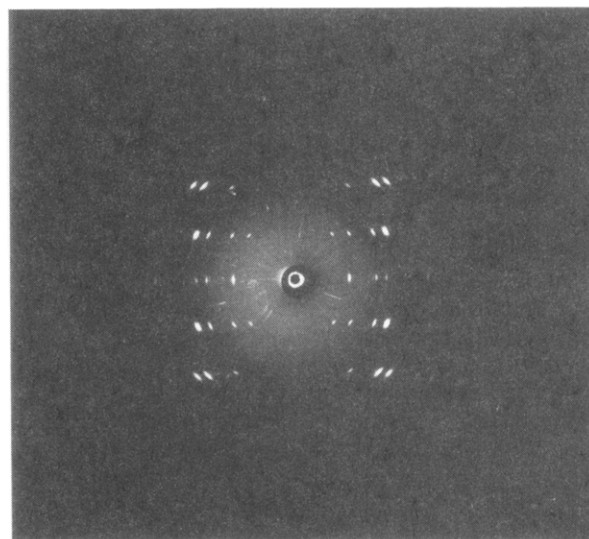


Figure 7. Wide-angle X-ray pattern of a stretched sample of the PEO-resorcinol molecular complex (α form). The stretching direction is vertical. The following intense reflections are observed: (a) on the layer line $l = 0$ (110), (200), (020), (120), (310); on the layer line $l = 1$ (011), (111), (201), (121), (221), (031), (401); on the layer line $l = 2$ (112), (022), (122), (222), (322), (312).

is given in Figure 7. Table II contains the experimental Bragg spacings of diffractions on the layer line $l = 0$ and the corresponding calculated spacings from the monoclinic unit cell, proposed by Myasnikova et al.¹³ Our values of the observed Bragg spacings do not agree closely with the calculated spacings of this monoclinic unit cell, where a large number of extinctions must be inferred. Therefore, we propose another unit cell, where a value of 0.984 nm for the c crystallographic parameter was determined from the position of the layer lines. From the values of 18 (hkl) Bragg spacings, an orthorhombic unit cell with $a = 1.050$ nm, $b = 1.018$ nm, and $c = 0.978$ nm is deduced. Table III contains experimental and calculated values of the reciprocal vector s_{hkl} from this orthorhombic unit cell. A good agreement is observed, and the number of extinctions is much lower. The volume of the unit cell is 1.040 nm³. The computed crystal density is 1.266 g/cm³, since the unit cell contains eight PEO monomer units and four resorcinol molecules. The density of the stretched sample of the molecular complex PEO-resorcinol is slightly lower (1.244 g/cm³), this is because the sample is not perfectly crystalline.

Unbanded Spherulite (α Form). The X-ray fiber pattern taken at the peripheral part of an unbanded spher-

Table II
Experimental and Calculated Bragg Spacings for
Reflections with $l = 0$

| experimental data | | indexation | | | |
|---------------------|----------------------------|-------------------|---------------------|--------------|---------------------|
| | | Myasnikova et al. | | our proposal | |
| d_{hkl}/nm | s^2_{hkl}/nm^{-2} | hkl | d_{hkl}/nm | hkl | d_{hkl}/nm |
| 0.7252 | 1.9015 | 200 | 0.7441 | 110 | 0.7291 |
| | | 020 | 0.7125 | | |
| 0.5238 | 3.0645 | 220 | 0.5146 | 200 | 0.5249 |
| 0.5061 | 3.9040 | 300 | 0.4960 | 020 | 0.5065 |
| 0.4550 | 4.8326 | 030 | 0.4750 | 120 | 0.4562 |
| | | 310 | 0.4685 | | |
| | | 130 | 0.4525 | | |
| 0.3305 | 6.9157 | 040 | 0.3562 | 310 | 0.3308 |
| | | 330 | 0.3431 | | |
| | | 140 | 0.3465 | | |
| | | 420 | 0.3298 | | |
| | | 240 | 0.3213 | | |
| 0.2865 | 12.1848 | 430 | 0.2929 | 320 | 0.2880 |
| | | 340 | 0.2894 | | |
| | | 500 | 0.2977 | | |
| | | 050 | 0.2850 | | |
| | | 510 | 0.2913 | | |
| | | 150 | 0.2799 | | |
| 0.2552 | 15.3566 | 250 | 0.2661 | 040 | 0.2533 |
| | | 440 | 0.2573 | 410 | 0.2541 |
| 0.2449 | 16.6765 | 530 | 0.2522 | 330 | 0.2430 |
| | | 350 | 0.2471 | 140 | 0.2462 |
| 0.2072 | 23.2857 | 550 | 0.2058 | 430 | 0.2072 |

Table III
Experimental Values of the Reciprocal Vector s_{hkl}

| hkl | $s \text{ obs}/\text{nm}^{-1}$ | $s \text{ calc}/\text{nm}^{-1}$ | hkl | $s \text{ obs}/\text{nm}^{-1}$ | $s \text{ calc}/\text{nm}^{-1}$ |
|-------|--------------------------------|---------------------------------|-------|--------------------------------|---------------------------------|
| 110 | 0.1379 | 0.1372 | 122 | 0.2996 | 0.2998 |
| 200 | 0.1909 | 0.1905 | 222 | 0.3410 | 0.3422 |
| 020 | 0.1976 | 0.1974 | 322 | 0.4038 | 0.4030 |
| 120 | 0.2198 | 0.2192 | 312 | 0.3641 | 0.3649 |
| 310 | 0.3026 | 0.3022 | 402 | 0.4299 | 0.4324 |
| 320 | 0.3491 | 0.3473 | 042 | 0.4418 | 0.4446 |
| 040 | 0.3919 | 0.3948 | 142 | 0.4552 | 0.4548 |
| 410 | | 0.3936 | 432 | 0.5239 | 0.5241 |
| 330 | 0.4084 | 0.4115 | 013 | 0.3227 | 0.3224 |
| 140 | | 0.4061 | 113 | 0.3364 | 0.3361 |
| 430 | 0.4826 | 0.4825 | 203 | 0.3611 | 0.3612 |
| 011 | 0.1433 | 0.1421 | 213 | 0.3744 | 0.3744 |
| 111 | 0.1722 | 0.1711 | 223 | 0.4100 | 0.4116 |
| 201 | 0.2164 | 0.2162 | 033 | 0.4260 | 0.4264 |
| 121 | 0.2405 | 0.2419 | 133 | 0.4352 | 0.4369 |
| 221 | 0.2927 | 0.2927 | 323 | 0.4619 | 0.4634 |
| 311 | 0.3170 | 0.3191 | 143 | 0.5063 | 0.5090 |
| 401 | 0.3923 | 0.3944 | 204 | 0.4513 | 0.4513 |
| 421 | 0.4377 | 0.4411 | 214 | 0.4614 | 0.4620 |
| 431 | 0.4930 | 0.4932 | 224 | 0.4891 | 0.4926 |
| 112 | 0.2471 | 0.2463 | 314 | 0.5087 | 0.5087 |
| 022 | 0.2842 | 0.2843 | | | |

ulite of the molecular complex PEO-resorcinol is shown in Figure 8. Examination of the experimental values for the Bragg spacings d_{hkl} of diffractions localized on the four first layer lines (Table IV) shows that unbanded spherulites have the same orthorhombic unit cell as stretched films. A plot of s^2_{hkl} for each set of diffractions having the same k and l Miller indices versus the square of the index (h) of the layer lines is given in Figure 9. The square root of the value of the slope obtained by linear regression gives the value of the a^* reciprocal parameter ($a^* = 1/1.052 \text{ nm}$), of the newly proposed orthorhombic unit cell. The a^* axis is along the spherulitic radii in unbanded spherulites. Unbanded spherulites and stretched films of the PEO-resorcinol molecular complex are in the same allotropic modification.

Space Group. The Miller indices of observed diffraction spots in the X-ray pattern, of stretched films of the PEO-resorcinol complex, are given in Table III. A

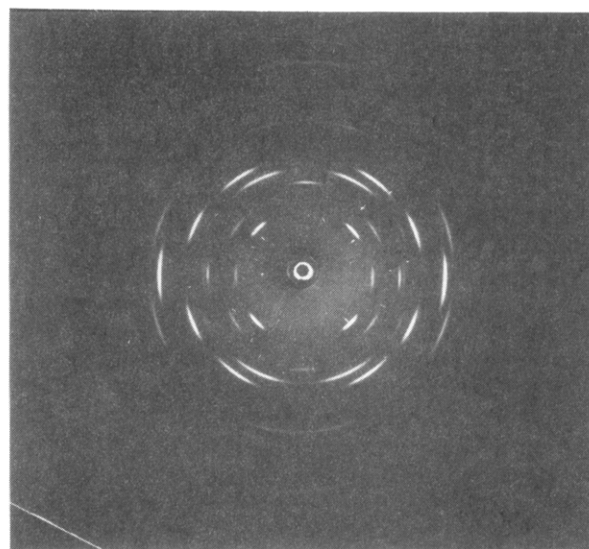


Figure 8. Wide-angle X-ray pattern obtained at the outline of a spherulite of the PEO-resorcinol molecular complex. The mean orientation of the spherulitic radius is vertical. The X-ray beam is perpendicular to the plane of the spherulite. The following intense reflections are observed: on the layer line $h = 0$ (011), (020), (002), (022); on the layer line $h = 1$ (110), (111), (120), (121), (122); on the layer line $h = 2$ (200), (201), (211); on the layer line $h = 3$ (310), (312).

systematic extinction is observed for $(0kl)$ diffractions when $(k + l)$ takes odd values. This implies, the presence of an n -glide plane, perpendicular to the a unit cell vector. For the $(h0l)$ reflections, a systematic extinction occurs for h odd (Table IV). This implies the existence of an a -glide plane perpendicular to the c unit cell vector. The 2_1 helical axes are parallel to the c crystallographic parameter and the proposed spatial group for the PEO-resorcinol crystalline molecular complex is $Pna2_1$. PEO chains may have a $4/1$ helical conformation with a pitch of 0.9776 nm (see next section).

Infrared Spectroscopy. The medium infrared spectra of the unbanded spherulite (Figure 10) and stretched film (Figure 11) are similar, which confirms again that both these samples belong to the same allotropic form.

Conformation of the PEO Molecule. The group symmetry of the PEO macromolecule in the helical conformation is either cyclic or dihedral.^{18,19} For dihedral symmetry, 9 and 20 IR-active modes are parallel and perpendicular, respectively. The possible conformations for a PEO helix belonging to the $D2\pi/4$ dihedral group can be deduced from the following equations derived by Miyazawa.²⁰

$$\cos(\theta/2) = \sin(\phi/2)[\sin \tau_{CO} \sin(\tau_{CC}/2) + \cos \phi \cos \tau_{CO} \cos(\tau_{CC}/2) + 2 \cos^2(\phi/2) \cos(\tau_{CC}/2)]$$

$$d \sin(\theta/2) = \sin(\phi/2)\{(r_{CC} + 2r_{CO}) \sin^2(\phi/2) \sin(\tau_{CO} + \tau_{CC}/2) - \cos^2(\phi/2)[2r_{CC} \sin(\tau_{CC}/2) + (2r_{CO} - r_{CC}) \sin(\tau_{CO} - \tau_{CC}/2)]\}$$

where d is the distance between each PEO monomer unit along the chain axis ($d = 0.2444 \text{ nm}$) and ϕ is the tetrahedral angle. Table V lists the values of the torsion angles τ_{CO} and τ_{CC} in addition to the distances of C, O, H1, and H2 atoms along the axis of the molecule for the four molecular models deduced from these equations. The corresponding projections of the PEO skeleton in the plane perpendicular to the chain axis are shown in Figure 12.

Table IV
Observed and Calculated Bragg Spacings and Their Indexation for the First Four Layer Lines of the X-ray Diffraction Pattern of a Spherulitic Sample of the PEO-Resorcinol Molecular Complex (α Form)^a

| layer line $h = 0$ | | layer line $h = 1$ | | layer line $h = 2$ | | layer line $h = 3$ | |
|---------------------|---------|---------------------|---------|---------------------|---------|---------------------|---------|
| d_{0kl}/nm | $(0kl)$ | d_{1kl}/nm | $(1kl)$ | d_{2kl}/nm | $(2kl)$ | d_{3kl}/nm | $(3kl)$ |
| 0.6980 | (011) | 0.7243 | (110) | 0.5224 | (200) | 0.3303 | (310) |
| (0.7035) | | (0.7291) | | (0.5249) | | (0.3308) | |
| 0.5072 | (020) | 0.5813 | (111) | 0.4608 | (201) | 0.3129 | (311) |
| (0.5065) | | (0.5845) | | (0.4625) | | (0.3135) | |
| 0.4909 | (002) | 0.4532 | (120) | 0.4181 | (211) | 0.2737 | (312) |
| (0.4988) | | (0.4562) | | (0.4208) | | (0.2740) | |
| 0.3499 | (022) | 0.4098 | (121) | 0.3530 | (202) | 0.2478 | (322) |
| (0.3518) | | (0.4135) | | (0.3577) | | (0.2481) | |
| | | 0.3312 | (122) | 0.3376 | (212) | | |
| | | (0.3335) | | (0.3373) | | | |
| | | | | 0.2908 | (222) | | |
| | | | | (0.2922) | | | |

^a Calculated lattice spacings d_{hkl} from the presently proposed orthorhombic unit cell are given in parentheses.

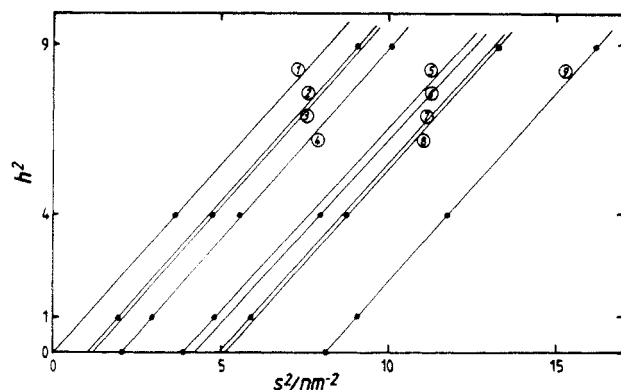


Figure 9. Square of the layer line number (h^2) versus s^2 for the diffractions found in the X-ray pattern of a spherulite sample (α form) of the PEO-resorcinol molecular complex: (1) ($h00$); (2) ($h10$); (3) ($h01$); (4) ($h11$); (5) ($h20$); (6) ($h02$); (7) ($h20$); (8) ($h12$); (9) ($h22$).

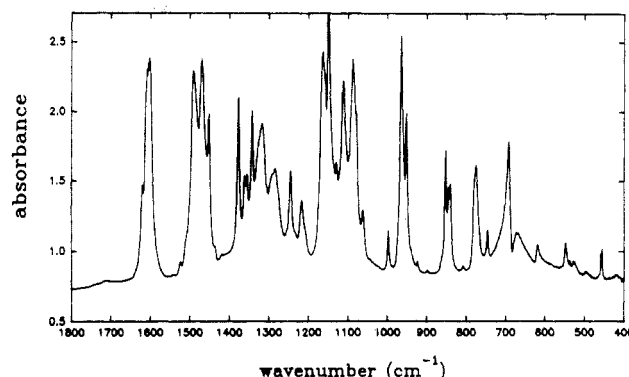


Figure 10. Medium infrared spectrum of unbanded spherulites of the PEO-resorcinol molecular complex (α form).

Table V
Torsion Angles and Radii of the Cylinder for Each Kind of PEO Helicoidal Chain

| model | τ_{CO}/deg | τ_{CC}/deg | r_C/nm | r_O/nm | r_{H1}/nm | r_{H2}/nm |
|-------|------------------------|------------------------|-----------------|-----------------|--------------------|--------------------|
| 1 | 110 | 10.85 | 0.1596 | 0.0356 | 0.0239 | 0.0218 |
| 2 | 103.8 | 194.92 | 0.1527 | 0.1912 | 0.0938 | 0.0250 |
| 3 | 182.8 | 54.56 | 0.1960 | 0.0931 | 0.2787 | 0.2436 |
| 4 | 49.7 | 94.37 | 0.0757 | 0.1420 | 0.1400 | 0.1376 |

Only the third of the calculated conformations is approximately trans-trans-gauche (TTG). The PEO vibration frequencies were calculated for these four conformational models using the GF-matrix method²¹ (Table VI). The observed vibration wavenumbers for the PEO-resorcinol molecular complex (α form), and the observed and calculated wavenumbers for pure crystalline PEO^{18,19} are

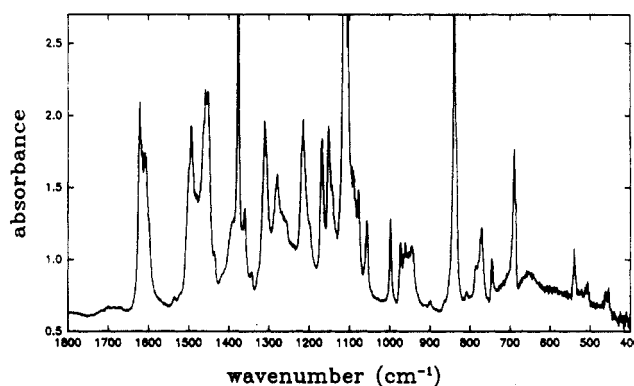


Figure 11. Medium infrared spectrum of a stretched film of the PEO-resorcinol molecular complex (α form).

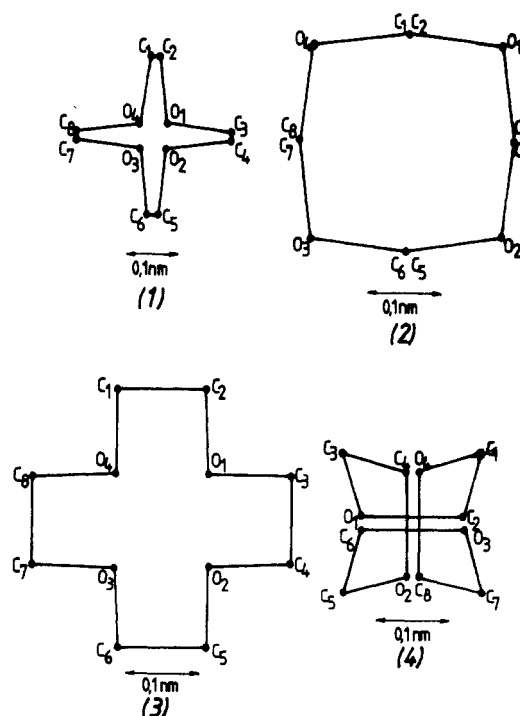


Figure 12. Projections in the plane perpendicular to the chain axis of the four hypothetical conformations deduced from Miyazawa's equations.

also given in Table VII. The models labeled 1 and 4 can be discarded because of large differences between observed and calculated wavenumbers. Model 3 possesses a nearly TTG conformation, and the calculated wavenumbers are nearly equal to those calculated for a 7/2 helical model. The lack of precision in our calculations does not allow us

Table VI
Calculated and Experimental Vibration Wavenumbers for the PEO and PEO-Resorcinol Complex

| model | | | | PEO | | |
|----------------------------|------|------|------|-------------------|------|------------------|
| 1 | 2 | 3 | 4 | molecular complex | exp | calc (7/2 helix) |
| Perpendicular Polarization | | | | | | |
| 2991 | 2943 | 2939 | 3034 | 2945 | | 2938 |
| 2974 | 2930 | 2932 | 2999 | 2916 | | 2933 |
| 2958 | 2891 | 2888 | 2938 | 2894 | | 2888 |
| 2922 | 2869 | 2872 | 2908 | 2878 | | 2872 |
| 1648 | 1459 | 1459 | 1751 | | 1466 | 1459 |
| 1631 | 1457 | 1456 | 1714 | 1452 | 1451 | 1456 |
| 1456 | 1370 | 1408 | 1418 | 1418 | 1411 | 1408 |
| 1370 | 1362 | 1357 | 1388 | 1362 | 1361 | 1353 |
| | | | | 1335 | 1350 | |
| 1332 | 1295 | 1284 | 1285 | 1284 | 1282 | 1283 |
| 1026 | 1263 | 1249 | 1173 | | 1234 | 1253 |
| 938 | 1108 | 1133 | 1073 | 1139 | 1147 | 1129 |
| | | | | 1133 | | |
| 912 | 1101 | 1095 | 1043 | 1133 | 1116 | 1098 |
| 735 | 1023 | 1036 | 935 | 1062 | 1063 | 1035 |
| 600 | 979 | 937 | 799 | 959 | 947 | 920 |
| 565 | 790 | 830 | 593 | 840 | 844 | 842 |
| | | | | 845 | | |
| 467 | 522 | 518 | 418 | (529) | 532 | 514 |
| 394 | 398 | 360 | 322 | 367 | 373 | |
| | | | | 352 | | |
| 230 | 286 | 204 | 147 | 240 | 217 | 209 |
| 141 | 120 | 136 | 123 | | 166 | 157 |
| 117 | 65 | 90 | 105 | | 93 | |
| Parallel Polarization | | | | | | |
| 2973 | 2929 | 2939 | 2998 | 2933 | | 2938 |
| | | | | 2916 | | |
| 2958 | 2891 | 2887 | 2907 | 2894 | | 2888 |
| | | | | 2878 | | |
| 1648 | 1459 | 1456 | 1714 | (1452) | 1462 | 1456 |
| | | | | | 1455 | |
| 1428 | 1371 | 1392 | 1414 | 1342 | 1342 | 1390 |
| 1062 | 1254 | 1287 | 1148 | 1245 | 1240 | 1284 |
| 950 | 1094 | 1045 | 973 | 1086 | 1103 | 1053 |
| | | | | 1090 | | |
| 602 | 961 | 863 | 683 | 952 | 958 | 881 |
| | | | | 924 | | |
| 404 | 451 | 570 | 353 | (332) | 530 | 539 |
| | | | | | 509 | |
| 106 | 116 | 105 | 105 | | 107 | 104 |

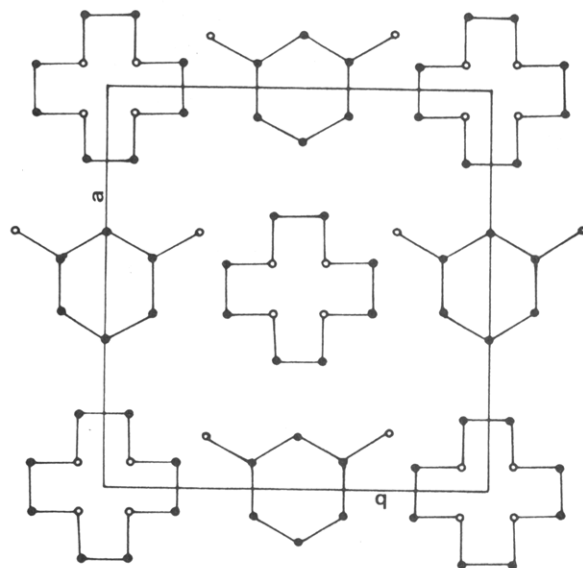


Figure 13. Projections of the unit cell of the α form of the molecular complex in the ab crystallographic plane.

to discriminate between models 2 and 3. Let us note that, as in the case of pure PEO (Table VI), the assumption of an helical conformation is, by necessity, an approximation.

Orientation of the Resorcinol Molecules in the Unit Cell of the Molecular Complex. The group symmetry

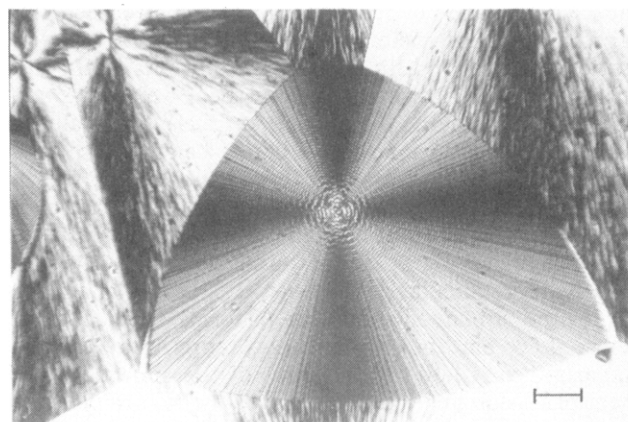


Figure 14. Optical micrograph (crossed polaroids) showing mainly banded spherulites of the PEO-resorcinol complex obtained from crystallization from the melt between two glass surfaces. The scale bar is 200 μm . The PEO molecular weight is 6000.

of the resorcinol molecule is C_{2v} . As a first approximation, the assignments of normal modes of vibration of resorcinol are taken according to Varsanyi²² and are improved upon using experimental values of the dichroic ratios obtained from polarized spectra. A stretched film and an unbanded spherulite, are used to determine the orientation of the resorcinol molecules with respect to the c and a

Table VII
Adsorption Bands of Resorcinol in the Molecular Complex
PEO-Resorcinol

| wavenumber/cm ⁻¹ | | attribution of Varsanyi |
|-----------------------------|---------|-------------------------|
| resorcinol | complex | |
| 458 | 457 | 16b (B ₁) |
| | 460 | |
| 545 | 538 | 6a (A ₁) |
| 682 | 693 | 4 (B ₁) |
| 748 | 746 | 1 (A ₁) |
| 768 | 776 | 11 (B ₁) |
| 855 | 852 | 17b (B ₁) |
| 962 | 965 | 7b (B ₂) |
| 1001 | 998 | 12 (A ₁) |
| 1162 | 1164 | 9b (B ₂) |
| 1490 | 1492 | 19b (B ₂) |

| wavenumbers/ cm ⁻¹ | <i>R</i> (A ₁ /A ₁ [⊥]) (stretched film) | <i>R</i> (A ₁ /A ₁ [⊥]) (spherulite) | normal mode |
|----------------------------------|---|---|-----------------------|
| 460 | 11.3 | ⊥ | 16b (B ₁) |
| 693 | 2.26 | 0.18 | 4 (B ₁) |
| 746 | 3.38 | *745 () 747 (⊥) | 10b (B ₁) |
| 776 | *774 () 780 (⊥) | 0.36 | 11 (B ₁) |
| 852 | | ⊥ | 17b (B ₁) |
| 457 | 0.16 | 0.25 | 15 (B ₂) |
| 965 | 0.1 | ⊥ | 7b (B ₂) |
| 1164 | | 0.25 | 9b (B ₂) |
| 1492 | ⊥ | 0.5 | 19b (B ₂) |
| 538 | 0.04 | 19.0 | 6a (A ₁) |
| 998 | 0.16 | | 18a (A ₁) |

crystallographic parameters. The deuterated PEO-resorcinol molecular complex was used to assign unambiguously the absorption bands due to the polymer and the guest molecule. Table VII (top) lists values for the wavenumbers of the resorcinol absorption bands found in the unpolarized IR spectra, of pure resorcinol and the complex in addition to Varsanyi's assignments. The band observed at 460 cm⁻¹ in the molecular complex was not reported by Varsanyi. Table VII (bottom) lists the measured dichroic ratios from a stretched film and from a spherulitic sample of the molecular complex and the indexation of the absorption bands of resorcinol. For the stretched film, absorption bands belonging to the A₁ and B₂ representations correspond to in-plane vibrations with their transition moments oriented along the 2-5 axis (or Z axis) and perpendicular to the 2-5 axis, respectively. Values of the dichroic ratio for several bands belonging to these representations indicate that these bands are perpendicularly polarized. Absorption bands belonging to the B₁ representation are out-of-plane vibrations and are parallelly polarized. The plane of the benzene ring is therefore nearly perpendicular to the fiber axis, i.e. the chain axis.

For the unbanded spherulite (α form), the absorption band at 538 cm⁻¹ belongs to the A₁ representation and is polarized parallelly to the radius of the spherulite. Vibrations belonging to the B₁ and B₂ modes are polarized perpendicularly in the spherulite. Therefore, the 2-5 axis of the resorcinol molecule is perpendicular to the (100) plane and the benzene ring is nearly perpendicular to the c axis of the unit cell (Figure 13). Additional work such as energy minimization of the proposed conformation of the PEO-resorcinol molecular complex is still in progress. As an additional remark, let us note a second discrepancy with the Varsanyi's assignments for resorcinol: from our experimental values of the dichroic ratio, the 10b mode belongs to the B₂ mode and not to the A₁ mode as proposed by Varsanyi. The vibrations at 746 cm⁻¹ for the spherulite and 776 cm⁻¹ for the stretched film are split in the corresponding polarization spectra (Table 7 (bottom)).

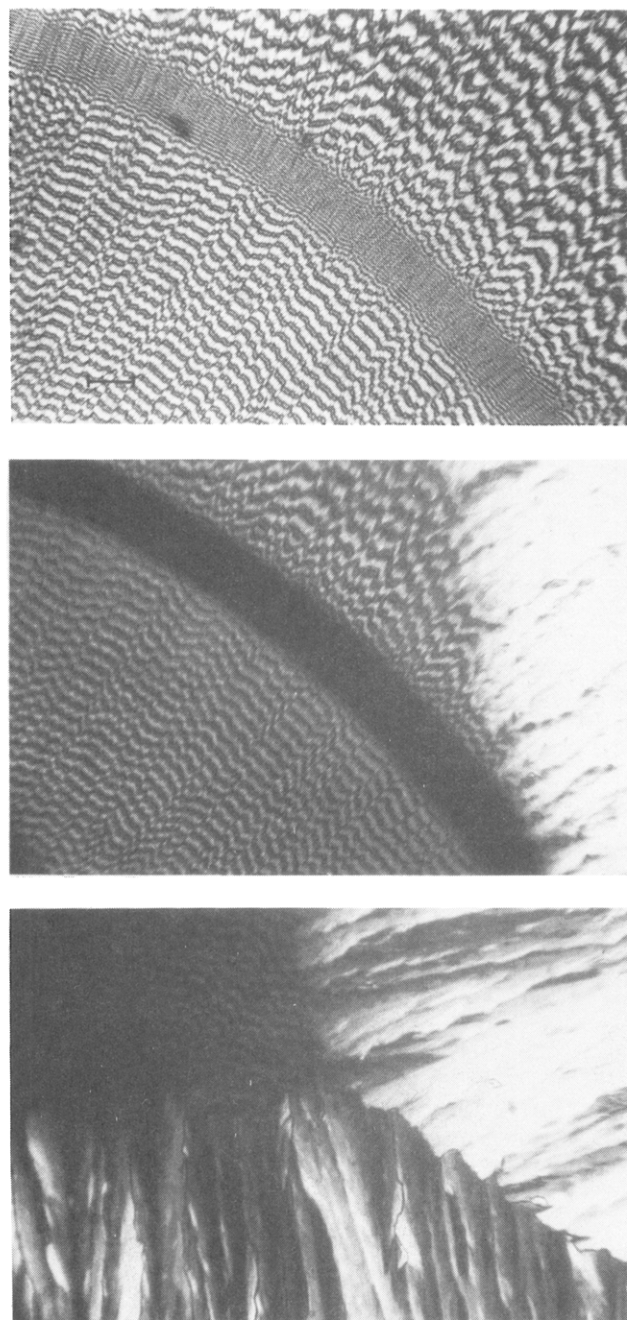


Figure 15. Influence of the crystallization and annealing temperature on banded spherulites (β form) crystallized step by step at various temperatures: (a, top) crystallization temperatures 40 °C (1), 25 °C (2), 45 °C (3); (b, middle) banded spherulites, crystallized at 25 °C, melted; (c, bottom) banded spherulites partially melted. The scale bar is 100 μm.

These shifts in wavenumbers occur because the molecules of resorcinol are inbedded in a crystalline environment.

As a conclusion, the 2-5-axis (or Z-axis) of the resorcinol molecule is perpendicular to the (100) crystallographic plane and the benzene ring lies in a plane nearly perpendicular to the c unit cell axis (chain axis).

Metastable Form of the Molecular Complex (β Form). Optical Microscopy. In addition to the α unbanded spherulite, the complex may also crystallize as banded spherulites in which the crystals of the molecular complex have another allotropic form (β form). Figure 14 shows an optical micrograph of these spherulites, with quasi circular extinction lines. Between crossed polaroids, banded spherulites reveal a dark Maltese cross pattern along the vibration directions of the polarizer and the

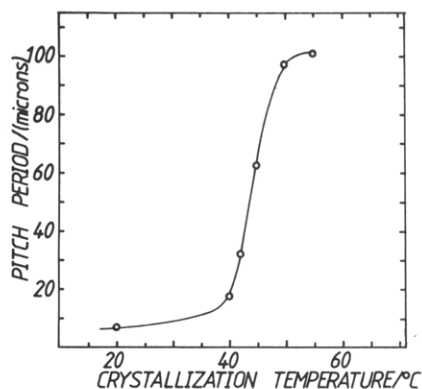


Figure 16. Pitch period for banded spherulites (β form) versus the crystallization temperature.

analyzer¹⁷ with alternating circular narrow positively and wide negatively birefringent bands, separated by the extinction lines (Figure 14). This double-ringed extinction pattern is caused by a periodic variation of the orientation of the crystals along the radius. As the medium optical index n_m of the crystals is along the radius of the spherulite, the large index n_g , the small index n_p , and one of the optical axes are along the microscope axis, respectively, in the center of the positively birefringent, negatively birefringent, and extinction bands. The value of the angle between the optical axes is 38° . Double-ringed spherulites of the PEO-resorcinol molecular complex are thus characterized by a positive biaxial indicatrix, taking into account that the large index n_g is the acute bisectrix of the angle between the optical axes.²³

The following experiments give a first insight to the dependence of structure and thermodynamic properties of this β phase on the crystallization temperature. Figure 15a illustrates that the pitch of the twist depends on the crystallization temperature. During the growth of a large β spherulite, the crystallization temperature is successively raised to 42°C and then lowered to 25°C and finally raised to 45°C . The ring spacing depends upon the crystallization temperature being larger the higher the temperature (Figure 16), as usually observed in polymers.^{17,24,25} Parts b and c of Figure 15 show that the thermodynamic properties of the β phase depend also on the crystallization temperature. On heating the sample shown in Figure 15a, melting of the β spherulite grown at 25°C is first observed (Figure 15b). Then the other portions of the spherulite recrystallize, without apparent melting, into the α form, as was previously suggested by Figure 15c and proved hereafter by FTIR spectroscopy.

The boundaries between spherulites of the same type are portions of hyperbolas with a small degree of curvature when the growth of two adjacent spherulites is nucleated approximately at the same time (Figure 6). Figure 17 is an optical micrograph showing both α and β spherulites grown at room temperature and their common boundary. As the growth rates of the α and β spherulites are different, the border is made of an arc of Descartes' oval connected to two arcs of logarithmic spiral, as previously explained by one of us:¹⁷ each point P of the arc of Descartes' oval AA' (Figure 18a) is simultaneously reached by both spherulites. Therefore

$$C_\alpha P/G_\alpha - t_\alpha = C_\beta P/G_\beta - t_\beta$$

where G_α and G_β are the growth rates for the α and β spherulites, respectively, and t_α and t_β are the times when they are nucleated. This equation is the bipolar equation of a Descartes oval. Only the points of the arc AA' of this oval may be reached by the crystallization initiated in C_α ,

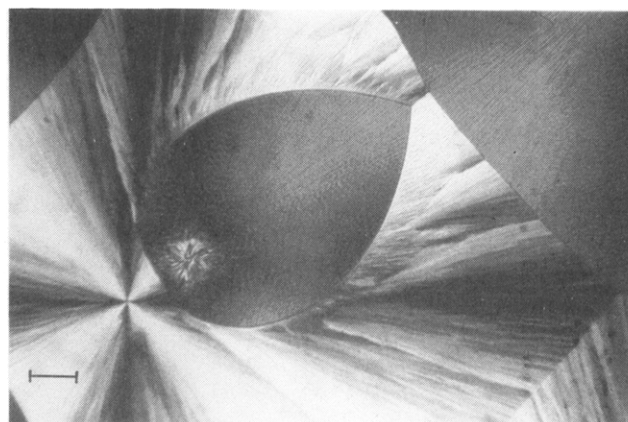


Figure 17. Border curves between different types of spherulites of the PEO-resorcinol molecular complex. The scale bar is $100\ \mu\text{m}$.

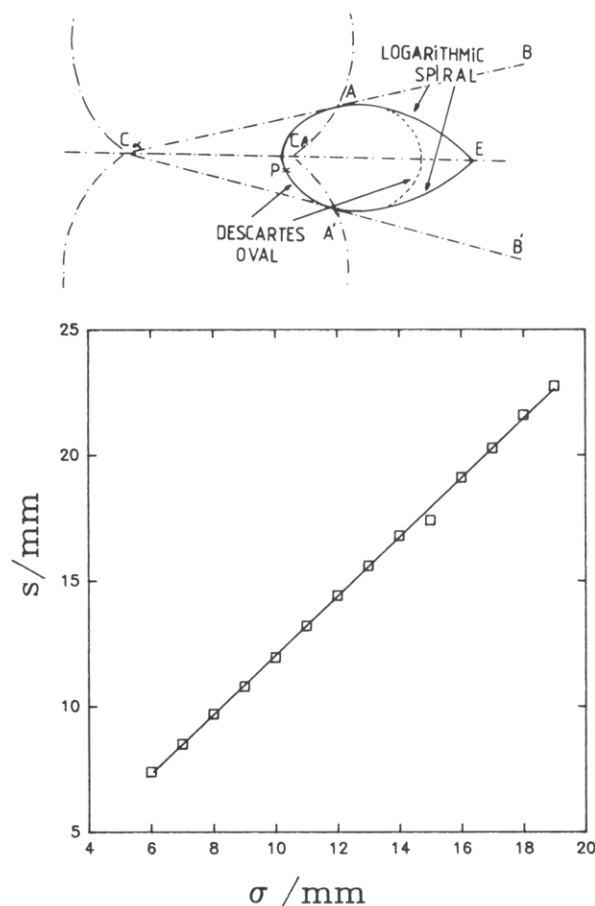


Figure 18. (a, Top) schematic drawing of the border of a β spherulite showing the Descartes' oval and the two arcs of the logarithmic spiral. (b, Bottom) linear relation between the length s of the arc of the logarithmic spiral and the radius σ of the spherulite.

and this arc is followed by the arcs of logarithmic spirals AE and A'E. The differential equation of the arc AE is

$$ds = (G_\alpha/G_\beta) d\sigma$$

where $\sigma = C_\beta P$, is the radius in polar coordinates with C_β as center, and s is the length of the arc of the curve. This equation is exactly verified in Figure 18b, which shows the graph of the length of the arc of the curved boundary; s is a linear function of σ with a value of 0.99994 for the coefficient of regression. It appears that the crystallization of the α form progresses along the arc AE with a rate G_α . The radial growth of the β spherulite is G_β . In cone $C_\alpha AA'$

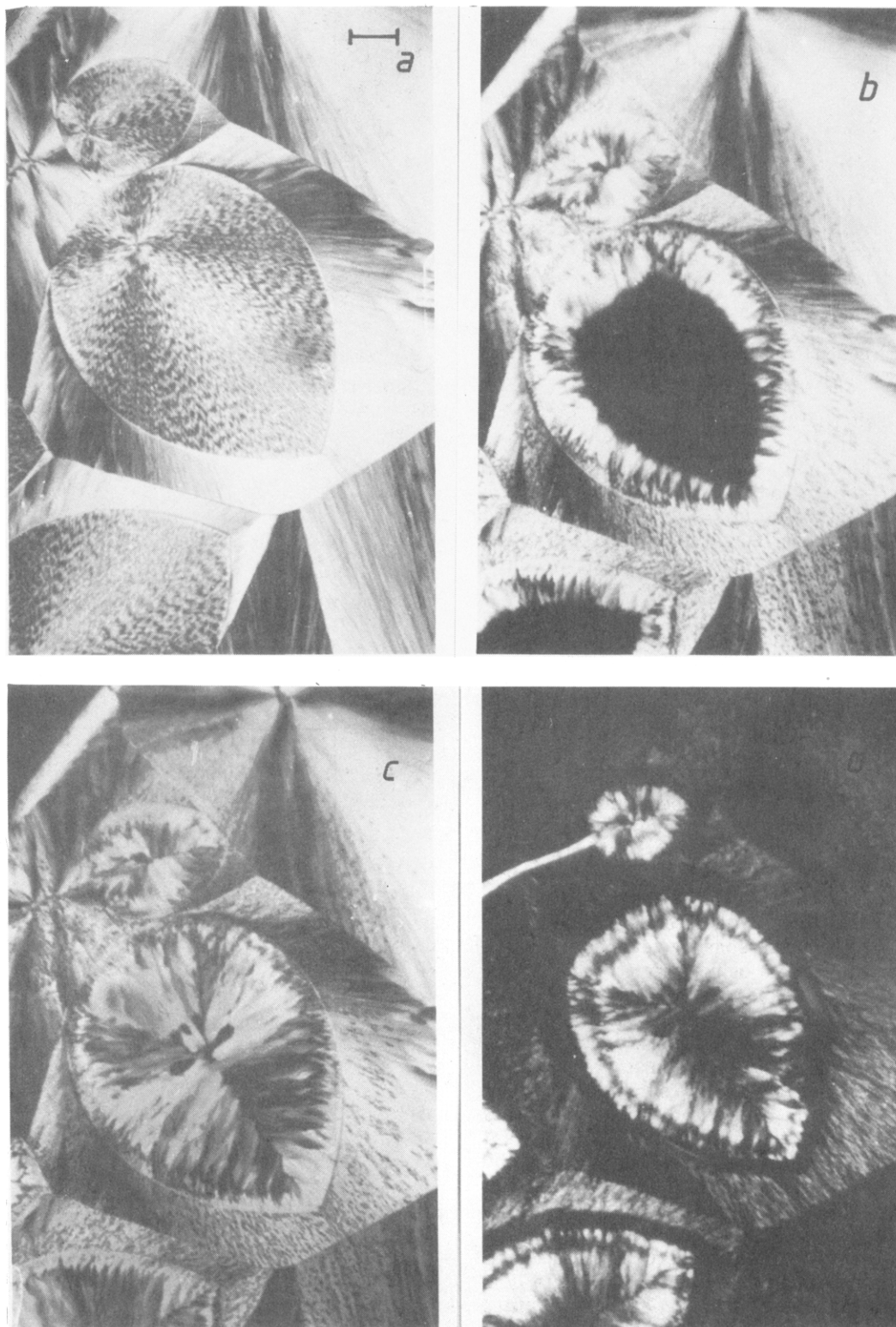


Figure 19. Influence of a progressive increase of temperature on β type spherulites: (a) micrograph showing banded (β form) and unbanded (α form) spherulites crystallized from the melt at room temperature; (b) temperature raised to 85 °C, banded spherulite partially melted; (c) recrystallization achieved in a few minutes; (d) at 94.6 °C (the final melting begins and ends at 95.5 °C). The scale bar is 100 μm .

and at large distances from C_α ("after" the β spherulite), the structure of the α spherulite is irregular. The idea that each point reached by the crystallization front is a center of radial crystallization appears here as a mathematical idealization. The morphology of real spherulitic systems is readily too complicated²⁶ to justify such an oversimplification. However, only minute changes in the orientation of the α crystals occur in a finite length along the arc of the logarithmic spiral and, along this arc, such

as approximation is valid, as shown from Figure 18b.

The transformation of the β spherulite form on rapid heating is shown in Figure 19. When the temperature of the sample approaches 80 °C, the β spherulites melt and then recrystallize into the α modification. Upon further heating, melting of the α spherulites occurs between 94.8 and 95.5 °C, as already mentioned in the section devoted to the α form. Figure 20 is an optical micrograph showing a banded spherulite, more or less largely transformed into

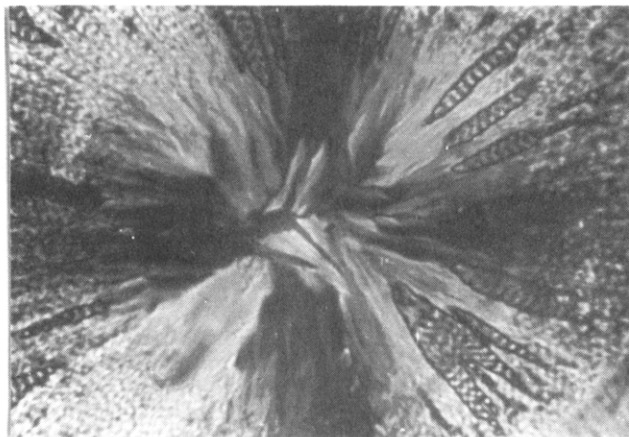


Figure 20. Banded spherulites (β form) partially transformed into the α form at room temperature.

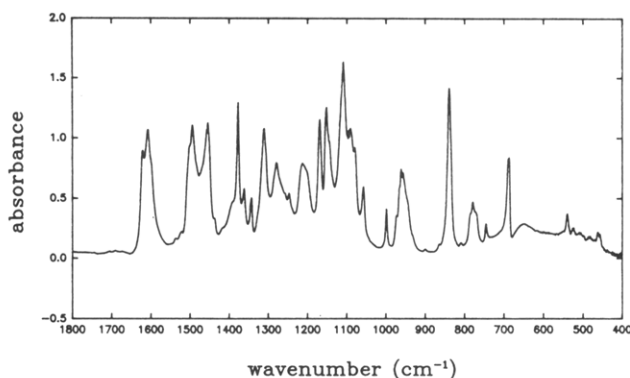


Figure 21. Medium infrared spectrum of banded β spherulites of the PEO-resorcinol molecular complex.

unbanded parts at room temperature. A kinetic study of this phase modification and the kinetic study on the spherulitic growth of the α and β forms of the PEO-resorcinol molecular complex and of solid-phase transformation shall be discussed elsewhere.

X-ray Diffraction. Unfortunately, a conventional X-ray source does not allow us to record the X-ray pattern of the β form spherulites of the molecular complex because of thickness limitations in sample preparation and its metastable behavior. At room temperature, the lifetime of β spherulites sandwiched between polypropylene films does not exceed 15 min. Use of synchrotron radiation is planned.

Fourier Transform Infrared Spectroscopy. The medium infrared spectra (medium IR) of the banded (β form) and annealed banded spherulites of the PEO-resorcinol molecular complex are given in Figures 21 and 22, respectively. The comparison of Figures 22 and 10 shows (a) the absorption bands at 507, 850, 1205, and 1392 cm^{-1} observed in the IR spectrum of banded spherulites (Figure 22) are not observed in the IR spectrum of unbanded spherulites (Figure 10) and (b), furthermore, the absorption bands of 619, 672, 845, 1133, 1235, 1293, 1304, 1356, and 1408 cm^{-1} observed in the IR spectrum of unbanded spherulites (Figure 10) are not observed in the IR spectrum of banded spherulites (Figure 21). Such large differences in the IR spectra for both types of spherulites, give an additional support to the existence of two allotropic modifications for the molecular complex. In the β allotropic form, large shifts even in the wavenumbers of the vibrations of resorcinol are observed. Moreover, the medium IR spectra of annealed banded spherulites (Figure 22) and unbanded spherulites (Figure 10) are similar. This last result is an additional proof of the metastability of

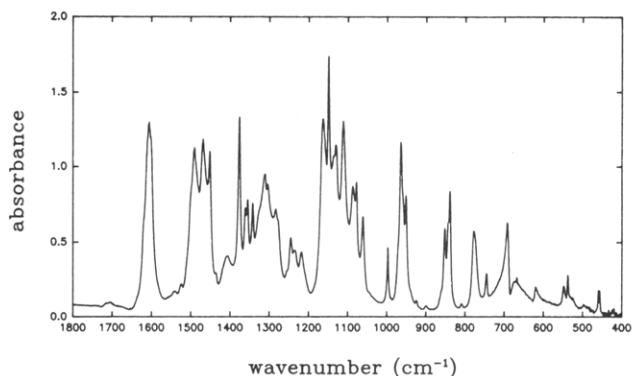


Figure 22. Medium infrared spectrum of banded β spherulites of the PEO-resorcinol molecular complex recrystallized by annealing.

the β form of the PEO-resorcinol molecular complex: annealed banded spherulites recrystallize as unbanded spherulites in the α form.

Conclusion

Differential scanning calorimetry, and optical microscopy show that the PEO-resorcinol molecular complex crystallizes into two allotropic forms called α and β . The β form is reported for the first time. The α form of the molecular complex melts at 93 $^{\circ}\text{C}$. The α form crystallizes as unbanded spherulites. The heat of complexation from the solid components is 10.16 kJ/mol of resorcinol. The wide-angle X-ray patterns of a stretched film and of spherulitic samples of the PEO-resorcinol molecular complex (α form) cannot be indexed with the monoclinic unit cell reported by Myasnikova et al.¹³ An orthorhombic unit cell with the parameters $a = 1.050$ nm, $b = 1.013$ nm, and $c = 0.9776$ nm with a $Pna2_1$ spatial group is proposed which accounts well for the experimental values of the Bragg spacings as well as the positions of the diffraction spots in both fiber type oriented diffraction patterns. The fiber axis is along the c parameter in stretched films and along the a parameter in spherulitic samples. From IR data, it is shown that in the stable form of the molecular complex, the 2-5 axis (or Z axis) of the resorcinol molecule is along the a^* parameter of the reciprocal lattice. The plane of the benzene ring of the resorcinol molecule is nearly perpendicular to the c axis.

The existence of another allotropic form (β form) of the PEO-resorcinol molecular complex has been demonstrated by optical microscopy, differential scanning calorimetry, and Fourier transform infrared spectroscopy. The melting temperature of the β form of the molecular complex is 71 $^{\circ}\text{C}$. This β form crystallizes as double-ringed spherulites which are metastable with respect to the α form and transform into the unbanded spherulites (α form) without apparent melting. Experimental evidence for this phase transformation has been obtained by optical microscopy and Fourier transform infrared spectroscopy.

Acknowledgment. We thank the "Fonds National de la Recherche Scientifique" for partial financial support.

References and Notes

- (1) Tadokoro, H.; Yoshibara, T.; Chatani, Y.; Murahashi, S. *J. Polym. Sci.* **1964**, *B2*, 363.
- (2) Tadokoro, H. *Macromol. Rev.* **1967**, *1*, 119.
- (3) Iwamoto, R.; Saito, Y.; Ishihara, H.; Tadokoro, H. *J. Polym. Sci.* **1968**, *A2*, 1509.
- (4) Yokoyama, M.; Ishihara, H.; Iwamoto, R.; Tadokoro, H. *Macromolecules* **1969**, *2*, 184.

- (5) Fenton, D. E.; Parker, J. M.; Wright, P. V. *Polymer* **1973**, *14*, 589.
- (6) Wright, P. V. *Br. Polym. J.* **1975**, *7*, 319.
- (7) Chatani, Y.; Okoyama, *Polymer* **1987**, *28*, 1815.
- (8) Point, J.-J.; Coutelier, Cl. *J. Polym. Sci., Polym. Phys. Ed.* **1985**, *23*, 231.
- (9) Point, J.-J.; Jasse, B.; Dosière, M. *J. Phys. Chem.* **1986**, *90*, 3273.
- (10) Point, J.-J.; Demaret, J. Ph. *J. Phys. Chem.* **1987**, *91*, 797.
- (11) Point, J.-J.; Coutelier, Cl.; Villers, D. *J. Phys. Chem.* **1986**, *90*, 3277.
- (12) Point, J.-J.; Coutelier, Cl. *Bull. Soc. Chim. Belg.* **1986**, *95*, 605.
- (13) Myasnikova, R. M.; Titova, E. F.; Obolonkova, E. S. *Polymer* **1980**, *21*, 403.
- (14) Cheng, C.; Belfiore, L. A. Reprint of the American Chemical Society Meeting, Miami, September 1989; p 325.
- (15) Buckley, C. P.; Kovacs, A. J. *Colloid Polym. Sci.* **1976**, *254*, 695.
- (16) ACA Monograph, No. 5, *Crystal data determinative tables*, 2nd ed.; Donnay, J. D. H., Ed.; ACA Monograph No. 5; 1963; pp 395, 491.
- (17) Point, J.-J. *Bull. Acad. R. Belg.* **1956**, *41*, 974.
- (18) Miyazawa, T.; Fukushima, K.; Ideguchi, Y. *J. Chem. Phys.* **1962**, *37*, 2764.
- (19) Yoshikara, T.; Tadokoro, S.; Murashashi, S. *J. Chem. Phys.* **1964**, *41*, 2902.
- (20) Miyazawa, T. *J. Polym. Sci.* **1961**, *55*, 215.
- (21) Tadokoro, H. *Structure of crystalline polymers*; John Wiley and Sons: New York, 1979.
- (22) Varsanyi, G. *Assignments for vibrational spectra of seven hundred benzene derivatives*; Adam Hilger: London, 1974; Vols. 1 and 2.
- (23) Hartshorne, N. H.; Stuart, A. *Crystals and the polarizing microscope*; Edward Arnold (Publishers) Ltd.: London, 1970; p 122.
- (24) Keller, A. *Nature* **1952**, *169*, 913.
- (25) Lindenmeyer, P. H.; Holland, V. F. *J. Appl. Phys.* **1964**, *35*, 55.
- (26) Bassett, D. C. *CRC Crit. Rev. Solid State Mater. Sci.* **1984**, *12*, 97-163.

Registry No. PEO-resorcinol (complex), 110933-77-2.